Department of Physics and Astronomy

University of Heidelberg

Master thesis

in Physics

submitted by

(name and surname)

born in (place of birth)

(year of submission)

Simulating effective field theories

on a space-time lattice with coloured noise

This Master thesis has been carried out by Matteo Zortea

at the

Institute for Theoretical Physics in Heidelberg

under the supervision of

Prof. Jan M. Pawloski

and

Dr. Felipe Attanasio

(Titel in Deutsch): (Abstract in Deutsch, max. 200 Worte)

(Title in English): (abstract in english, at most 200 words)

Erklärung:

Ich versichere, dass ich diese Arbeit selbstständig verfasst habe und keine anderen als die angegebenen Quellen und Hilfsmittel benutzt habe.

Heidelberg, den 27.11.2023 ....

Contents

List of Figures

List of Tables

"Grazie a tutti."

Matteo Zortea

Chapter 1

Introduction and outline

1.1 Quantum chromodynamics and its and phase diagram

Big picture: here we talk about QCD and the problem of the phase diagram

1.2 Effective theories

Here we first define effective theories and discuss their usefulness, then introduce RG as a technique to resolve physics at different scales.
 Motivation for choices, connection to stochastic regularisation, complex langevin,

easy noise [**boo**]

Chapter 2

Theoretical background

In this chapter we want to provide with an overview on the general theoretical framework that supports this work, and introduce the main concepts for the successive parts. Each section in this chapter is, by no means, meant as an exhaustive treatment. The description will be quite conceptual, rather than technical, and aims at recalling the main ideas and fix conventions. We ask the reader to consult appropriate references, which will be given in the corresponding sections, for a more detailed treatment of the topics.

2.1 The renormalisation group

Landau's mean field approach to study phase transition [1] gained wide popularity in the 1930's and 40's, since it was able to describe critical properties of many systems and it provided inspiration for the later Landau-Ginzburg theory of superconductivity [2]. Thus, it was soon proved to be inaccurate to predict some experimentally well proven properties of certain systems near their critical point [3]. This is because, beeing a mean field theory, it did not take into account the role of spatial fluctuations. The idea of block-spin transformation, systematically developed by Kadanoff [4], made a big step towards a deeper understanding of the scaling behaviour, and posed the basis for the later work of Wilson [5–7], which still constitutes the basis for modern approaches to renormalisation in field theory and statistical physics.

2.1.1 Block-spin RG

To illustrate the idea, let us consider a set of spins whose magnetisation is described by a function $\phi(x)$. The spins are located on a discrete lattice $\mathscr{L}$ with spacing a, so that the function assumes values only at such sites $\phi(x_i) = \phi_i \neq 0 \Leftrightarrow x_i \in \mathscr{L}$. Suppose then that their interaction is described by a certain action $S[\phi]$ and a partition function

$$Z = \sum_{\phi} e^{-S[\phi]}.$$

We now want to introduce a coarse-grained (or blocked) field $\bar{\phi}$ within a spacetime cell of volume $\mathcal{V}$. Such a coarse grained field can be defined, for example, as an average over the spins within the cell $\mathcal{V}$. If the spins can only be 0 or 1 like in a Ising model, then we might opt for a majority rule [8]. We now want to find a new action S_b such that

$$Z = \sum_{\phi} e^{-S(\phi)} = \sum_{\bar{\phi}} e^{-S_b(\bar{\phi})}. \tag{2.1}$$

FIGURE 2.1: The two steps of the block-spin transformation. The black dots indicate the original field ϕ, while the blue dots indicate the coarse-grained field $\bar{\phi}$.

Suppose for the moment that such S_b has been found. The coarse-graining procedure comes with a loss of resolution since the spacing is changed $a \to 2a$. Hence one can rescale distances and momenta in the new action via $a \to a/2, p \to 2p$ and then compare the result with the initial action. This constitutes the second step of the block-spin transformation.

The whole procedure can be iterated multiple times, and can be thought as a zoom-out with a corresponding coarse graining, in order to describe the system in terms of the relevant scales as pictured in figure 2.1. As made clear in the picture, the physical correlation length ξ is reduced by the block-spin step, since the description is now in terms of the coarse field $\bar{\phi}$. There are only two exceptions for this, either the correlation length is zero, or infinite. The latter case represents a fixed-point of the RG, and the system exhibits scale invriance.

Note that the condition (2.1) is non-trivial. One can, in principle, build an ad-hoc action that fulfills the condition, but it is complicated, since S_b can be also be very different from S. For example, if the action $S[\phi]$ contains only nearest-neighbour interactions, the new action $S'[\bar{\phi}]$ can contain higher order interactions such as nearest-to-nearest neighbour, or even more. In principle, all the terms compatible with the original symmetries are allowed, and one has often to rely on some approximations. For example, if one is interested in long range properties of the system, and the volume $\mathcal{V}$ is sufficiently small, one can assume the functional form of the action S to remain approximately the same, with the the only change due to the dimensional rescaling of dimensionful quantities mentioned above. Thus, as the procedure is iterated and the correlation length scale is approached, one has to take account higher order interactions. For an example of the explicit construction of the RG for an Ising model, see [8].

2.1.2 Wilsonian RG

The Wilsonian picture of renormalisation [5, 6] is formulated in momentum space and in general is more suitable for theories in the continuum.

The idea is that a physical theory observed a energy scale Λ can be seen as an effective theory of a more fundamental one, defined at scale $\Lambda_0 > \Lambda$.

To see how this can happen, let us consider a theory defined by the action $S[\phi]$ scale Λ_0, and let us split the field as

$$\phi = \bar{\phi} + \varphi$$

where $\bar{\phi}$ are fields with momenta $p^2 \leq \Lambda^2$ and φ are fields with $\Lambda^2 < p^2 \leq \Lambda_0^2$.

This allows to split the action as

$$[\bar{\phi} + \varphi] = S_\Lambda[\bar{\phi}] + \delta S[\bar{\phi}, \varphi]$$

including all the dependence on φ in $\delta S[\bar{\phi}, \varphi]$.

The path integral can be rewritten as

$$Z = \int D\phi \, e^{-S[\phi]} = \int D\bar{\phi}_\Lambda \, e^{-S_\Lambda[\phi]} \int D\varphi \, e^{-\delta S[\phi, \varphi]}$$
$$= \int D\bar{\phi}_\Lambda \, e^{-S_\Lambda[\bar{\phi}] - S_{\text{UV}}[\bar{\phi}]}$$
$$= \int D\bar{\phi}_\Lambda \, e^{-S_\Lambda^{\text{eff}}[\bar{\phi}]},$$

where

$$S_\Lambda^{\text{eff}} = S_\Lambda[\bar{\phi}] + S_{\text{UV}}[\bar{\phi}], \qquad S_{\text{UV}}[\bar{\phi}] = -\log\left(\int D\varphi \, e^{-S_\Lambda[\phi, \varphi]}\right).$$

$S_{\text{UV}}[\bar{\phi}]$ encodes all the information of UV modes with $\Lambda^2 < p^2 \leq \Lambda_0^2$.

The action $S_\Lambda[\bar{\phi}]$ has the same functional form of the initial action $S[\phi]$, but it is now defined only for fields with momenta $p^2 \leq \Lambda^2$. Instead, $S_\Lambda^{\text{eff}}[\bar{\phi}]$ constitutes an effective description of the original theory at scale Λ and depends only on degrees of freedom with $p^2 \leq \Lambda^2$.

One can then operate a rescaling of distances and momenta to complete the Wilson RG step, according to the parameter

$$s^2 = \Lambda^2 / \Lambda_0^2.$$

If, for example, d_g is the energy dimension of a coupling g in the action, then the rescaling transformation causes

$$g \to s^{d_g} g.$$

The same applies to the fields and other dimensionful quantities. If the corrections from S_{UV} are negligible, such as for high cutoff $\Lambda \approx \Lambda_0$, then this is the only contribution to the change in the couplings and fields due to the Wilson step. More in general, for higher order iterations of the procedure, the couplings' dependence on s is caputered by the β-functions

$$\beta_g = \frac{d}{ds} g(s).$$

A full treatment of RG is out of scope here and we ask the reader to consult more appropriate references fore more details [9].

At this point, one can clearly see the analogy with the block-spin transformation introduced in the previous section. Performing the integral over high momenta modes can be thought as performing averages (coarse graining) over neighbours. This causes a loss of resolution which can be recovered by rescaling distances and momenta. The rescaling is essential for a description of fixed points, since it can be pictured as a zoom-out.

Therefore, the philosophy of Kadanoff and Wilson approaches was that the blocking transformation reduces the complexity of many-body systems by systematically reducing the number of degrees of freedom being taken into account, without changing the physical content of the theory [10, 11].

We want to conclude this section by mentioning that the splitting of the action can be done by writing

$$S_\Lambda^{\text{eff}}[\bar\phi] = S[\phi] + \Delta S_\Lambda^{(\text{IR})}[\bar\phi],$$

where $\Delta S_\Lambda^{(\text{IR})}[\hat\phi]$ is a regulating function which typically assumes the form

$$\Delta S_\Lambda^{(\text{IR})}[\bar\phi] = \frac{1}{2} \int \frac{\mathrm{d}^d p}{(2\pi)^d} \bar\phi(-p)\, \Lambda^2 \left(\frac{1}{r_\Lambda(p^2)} - 1 \right) \bar\phi(p), \qquad (2.2)$$

For a sharp momentum cutoff one has

$$r_\Lambda(p^2) = \theta\left(p^2 - \Lambda^2\right).$$

This result will allow for a deep connection between coloured stochastic quantisation and the functional renormalisation group, the latter describing the functional dependence of $S_\Lambda^{\text{eff}}[\bar\phi]$ on the cutoff scale Λ citationsssss.

2.2   Lattice QFT and the continuum limit

The starting set up is the euclidean formulation of quantum field theory, where one typically defines a path integral Z, which, for a general scalar field $\phi(x)$ and a fermion field $\psi(x)$, assumes the form

$$Z = \int \mathcal{D}\phi \mathcal{D}\psi \mathcal{D}\bar\psi\, e^{-S[\phi,\psi,\bar\psi]}, \qquad \mathcal{D}\xi = \prod_x d\xi_x, \quad \xi \in \{\phi, \psi, \bar\psi\}, \qquad (2.3)$$

and correlation functions are computed via

$$\langle \xi_{x_1} \dots \xi_{x_n} \rangle = \frac{1}{Z} \int \mathcal{D}\phi \mathcal{D}\psi \mathcal{D}\bar\psi\, \xi_{x_1} \dots \xi_{x_n}\, e^{-S[\phi,\psi,\bar\psi]}, \qquad \xi_{x_i} \in \{\phi_{x_i}, \psi_{x_i}, \bar\psi_{x_i}\}.$$

Let us then consider a lattice $\mathscr{L}$, with spacing a, and N_μ points in each spacetime direction μ, hence a physical length $L_\mu = N_\mu a$. For simplicity we restricted here to a scalar field ϕ and we will recall fermionic properties only when relevant, but what follows has general validity. The action and the path integral measure are now taken over discrete quantities

$$S = \int d^d x\, \mathcal{L}(\phi(x)) \qquad \rightarrow \qquad S = a^d \sum_{n \in \mathscr{L}} \mathcal{L}(\phi(n)),$$

$$\prod_x d\phi(x) \qquad \rightarrow \qquad \prod_{n \in \mathscr{L}} d\phi(n),$$

where $\mathcal{L}(\phi)$ is the Lagrangian density function.

The path integral is hence

$$Z = \int \prod_n d\phi(n)\, e^{-S[\phi]},$$

and the probability of a field configuration ϕ

$$p(\phi) = \frac{1}{Z}\, e^{-S[\phi]}. \tag{2.4}$$

Expectation value of observables are computes as

$$\langle O(\phi) \rangle = \frac{1}{Z} \int \prod_n d\phi(n)\, O(\phi)\, e^{-S[\phi]}. \tag{2.5}$$

In order to simulate a theory and perform the above sums one has to go to finite volumes and impose boundary conditions. In the space directions, we take periodic conditions

$$\phi(t, \vec{x}) = \phi(t, \vec{x} + \vec{T}),$$
$$\psi(t, \vec{x}) = \psi(t, \vec{x} + \vec{T}).$$

Instead, a finite time extent is related to the temperature of the system [12, 13] via

$$\beta = 1/T = 1/L_t,$$

and boundary conditions are chosen depending on the spin-statistic of the corresponding particles, namely periodic conditions for bosons, and anti-periodic for fermions

$$\phi(t, \vec{x}) = \phi(t + T, \vec{x}) \qquad \text{bosons,}$$
$$\psi(t, \vec{x}) = -\psi(t + T, \vec{x}) \quad \text{fermions.}$$

Such a formulation naturally brings a momentum cutoff $\Lambda = \pi/a$ since now all the momenta are restricted to the first Brilloune zone $p_\mu \in [-\pi/a, \pi/a]$.

To compute observables one relies on Monte-Carlo methods to generate field configurations, sampling the distribution (2.4) and convergence to the statistical value given by (2.5) is expected in the limit of infinite samples $N_{\text{samp}} \to \infty$.

To recover the continuum results, one has to take $V \to \infty, a \to 0$ [1], but this task cannot be done so straightforwardly. Continuum limits of lattice theories are intimately connected to the existence of critical points. To see why this is the case, consider the dimensionless mass gap

$$\hat{\xi} = m\, a$$

of a certain theory. The quantity ξ is also called correlation length and it is related to the exponential decay of correlation functions between local observables measured at different points on the lattice, as given by add ref. eq.

When taking the continuum limit we want $a \to 0$, while having a finite physical mass m. This implies that the correlation length $\hat{\xi}$ has to diverge: in the language of statistical physics, this is a second order phase transition. Of course to bring the system at its critical point, where such phase transition happens, one has to tune the bare parameters g_0^i of the theory to their critical values g_0^{i*}. To do this, one should

---

[1] the order here is important, see for example [14, 15]

find the zeros of the lattice beta functions

$$\beta_g^{\text{latt}} = a \frac{d}{da} g(a) \overset{!}{=} 0, \qquad a = \pi / \Lambda.$$

As this is quite hard task to do on the lattice, one typically relies on some approximation schemes such as employing perturbative continuum beta functions.
In any case, from this description it should be clear that the spacing a should not be treated as a free parameter in the continuum limit, but rather a dynamically determined quantity that depends on the couplings of the theory.

Note that in the limit $a \to 0$, one has $\Lambda \to \infty$. If one's scope is to simulate an effective theory which is expected to hold only up to a scale Λ_{phys}, one must have $\Lambda \leq \Lambda_{\text{phys}}$, with a consequent lower bound on the lattice spacing $a \geq a_{\text{phys}} = \pi / \Lambda_{\text{phys}}$.

2.3 Stochastic quantisation

The idea of stochastic quantisation [16, 17] is that Euclidean Quantum Field theory can be thought as a system in thermal equilibrium with a heat reservoir and hence described as a stochastic process via the Langevin equation. For this, one has to introduce a fictitious time variable τ that labels the state $\phi(\tau, x)$ of the system during the evolution.

2.3.1 Standard stochastic quantisation

Let us consider, for example, a scalar field ϕ with a Euclidean action $S[\phi]$ and the following Langevin equation

$$\partial_\tau \phi(\tau, x) = -\frac{\delta S[\phi]}{\delta \phi(\tau, x)} + \eta(\tau, x), \tag{2.6}$$

where $K_\phi(\tau) \equiv -\delta S[\phi]/\delta \phi(\tau, x)$ is the drift term and $\eta(\tau, x)$ is a random white noise field assumed to be normally distributed

$$P(\eta) = \frac{\exp\left(-\frac{1}{4} \int_{\tau,x} \eta^2(\tau, x)\right)}{\int D\eta \exp\left(-\frac{1}{4} \int_{\tau,x} \eta^2(\tau, x)\right)},$$

which, in particular, implies

$$\langle \eta(x, \tau) \rangle = 0, \qquad \langle \eta(x, \tau) \, \eta(x', \tau') \rangle = 2 \, \delta(x - x') \, \delta(\tau - \tau'). \tag{2.7}$$

Stochastic average with respect to the measure $P(\eta)$ are computed via

$$\langle A(\eta) \rangle = \int D\eta \, P(\eta) \, A(\eta).$$

In momentum space, (2.7) becomes

$$\langle \eta(p, \tau) \rangle = \left\langle \int_x e^{ipx} \eta(x, \tau) \right\rangle = \int_x \left\langle e^{ipx} \eta(x, \tau) \right\rangle = 0,$$

$$\langle \eta(p, \tau) \eta(q, \tau') \rangle = \left\langle \int_{xy} e^{ipx+iqy} \eta(x, \tau) \eta(y, \tau') \right\rangle$$

$$= \int_{xy} e^{ipx+iqy} \left\langle \eta(x, \tau) \eta(y, \tau') \right\rangle \qquad (2.8)$$

$$= 2 (2\pi)^2 \delta(p+q) \delta(\tau - \tau').$$

In absence of the noise term $\eta(\tau, x)$, equation (2.6) simply represents an evolution of the field towards the minimum of the action, and at equilibrium the field is constrained to $\partial_\tau \phi(x, \tau) = 0 = \delta S[\phi]/\delta\phi(\tau, x)$, namely to the classical equations of motion.

For any observable O, which is function of the field, one has, for fixed time τ,

$$\langle O(\phi(\tau)) \rangle = \int D\eta \, P(\eta) \, O(\phi(\tau)),$$

from which it follows straightforwardly using the Langevin equation and $\langle \eta \rangle = 0$

$$\frac{d}{d\tau} \langle O(\phi(\tau)) \rangle = \left\langle \frac{\delta O}{\delta\phi(\tau, x)} \partial_\tau \phi(\tau, x) \right\rangle = - \left\langle \frac{\delta O}{\delta\phi}(\tau, x) \frac{\delta S}{\delta\phi(\tau, x)} \right\rangle.$$

It follows trivially that for $O(\phi(\tau)) = \phi(\tau, x)$

$$\frac{d}{d\tau} \langle \phi(\tau, x) \rangle = - \left\langle \frac{\delta S}{\delta\phi(\tau, x)} \right\rangle \xrightarrow[Equilibrium]{} \left\langle \frac{\delta S}{\delta\phi(\tau, x)} \right\rangle = 0.$$

This also provides a consistency check for the correct implementation of the simulation, since the drift $K_\phi = -\delta S/\delta\phi$ is computed numerically during the evolution. More generally, one can derive a correspondent Fokker-Planck equation [18], which can be proven to have a stationary distribution if the action is bounded from below, given by [17]

$$\mathcal{P}(\phi) = \frac{1}{Z} \exp\left(-S[\phi]\right). \qquad (2.9)$$

This allows one to compute correlation functions as moments of the probability distribution (2.9). In particular, one has

$$\langle O \rangle_{P(\eta)} = \langle O \rangle_{\mathcal{P}(\phi)} \equiv \langle O \rangle. \qquad (2.10)$$

2.3.2 Stochastic quantisation with coloured noise

In the stochastic quantisation procedure the noise which accounts for the quantum fluctuations of the theory is assumed to be white, as defined in equations (2.7), (2.8). We now want to examine the dynamics in presence of a coloured noise, writing the Langevin equation as

$$\partial_\tau \phi(x, \tau) = - \frac{\delta S[\phi]}{\delta\phi(\tau, x)} + \eta_{\text{col}}(x, \tau),$$

with $\eta_{\text{col}}(x, \tau) = r_\Lambda(x)\,\eta(x, \tau)$. In particular, here we restrict to the regulating function defined as a sharp cutoff in momentum space

$$r_\Lambda(p) = \theta(\Lambda^2 - p^2), \tag{2.11}$$

and we invite the reader to consult [19] for a discussion of other regulating functions. The noise field in momentum space is then

$$\begin{aligned} \eta_{\text{col}}(p, \tau) &= \mathcal{F}[\eta_{\text{col}}(x, \tau)] = \mathcal{F}[r_\Lambda(x, \tau)\eta(x, \tau)] = \mathcal{F}[r_\Lambda(x, \tau)] \star \mathcal{F}[\eta(x, \tau)] \\ &= \theta(\Lambda^2 - p^2)\,\eta(p, \tau). \end{aligned}$$

where $\mathcal{F}$ indicates the Fourier transform and $\star$ the convolution product.

An interesting quantity to look at is the position-space noise correlation function

$$\begin{aligned} C_\eta(x, \tau, y, \tau') &= \left\langle \eta_{\text{col}}(x, \tau)\,\eta_{\text{col}}(y, \tau') \right\rangle \\ &= \frac{1}{(2\pi)^4} \int D\eta\, P(\eta) \left[\int_{p,q} e^{-ipx - iqy} \eta_{\text{col}}(p, \tau)\,\eta_{\text{col}}(q, \tau') \right] \\ &= \frac{1}{(2\pi)^4} \int_{p,q} e^{-ipx - iqy} \int D\eta \left[P(\eta)\,\eta(p, \tau)\,\eta(q, \tau') \right] \\ &\quad \times \theta(\Lambda^2 - p^2)\,\theta(\Lambda^2 - q^2) \\ &= \frac{2}{(2\pi)^2} \int_{p,q} e^{-ipx - iqy}\, \delta(p + q)\,\theta(\Lambda^2 - p^2)\,\theta(\Lambda^2 - q^2)\,\delta(\tau - \tau') \\ &= \frac{2}{(2\pi)^2} \int_p e^{-ip(x-y)}\,\theta(\Lambda^2 - p^2) = \frac{1}{\pi} \int_0^\Lambda d\omega\,\omega\, J_0(\omega|x - y|), \end{aligned} \tag{2.12}$$

where $J_0(x)$ is a Bessel function of the first order. The integral in the last line is computed numerically as a function of $d = |x - y|$ and reported in figure 2.2 for three different values of the cutoff $\Lambda_1 < \Lambda_2 < \Lambda_3$. This shows nicely that for $|x - y| \ll 1/\Lambda$ the noise is now correlated, while for $|x - y| \gg 1/\Lambda$ the correlation function vanishes, as in the white noise case. In other words, only the short-length behaviour of the system is affected by the introduction of such a regulating term, as one could expect.

Another intuitive and interesting aspect of the dynamics in the presence of coloured noise can be deduce by looking at the field expression in terms of the retarded Langevin Green function [17], which is here not derived, but reported from [19]

$$\phi(x, \tau) = \int_{x'} \int_{-\infty}^\tau d\tau'\, G\left(x - x', \tau - \tau'\right) \left[r_\Lambda\left(\Delta_x\right) \eta\left(x, \tau'\right) - \frac{\delta S}{\delta \phi}\Big|_{p=0} \phi\left(x', \tau\right) \right],$$

where

$$G\left(x - x', \tau - \tau'\right) = \theta\left(\tau - \tau'\right) \int_p e^{-ip\cdot(x-x')} e^{-(\tau-\tau')\left(p^2 + m^2\right)}.$$

By looking at the first term in the square bracket, one can conclude that there is no propagation of modes with momentum $p^2 \geq \Lambda^2$ due to the noise term, but one can still have contribution from modes $p^2 > \Lambda^2$ from the second term, which corresponds to the deterministic part of the equations of motion. Stated differently, UV quantum fluctuations with $p^2 > \Lambda^2$ are removed from the dynamics of ϕ, but still contribute classically.
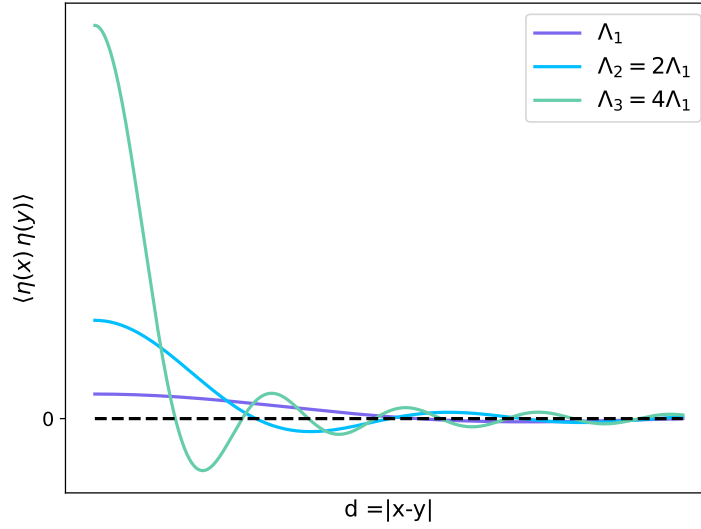
FIGURE 2.2: Noise correlation as a function of $d = |x - y|$ for three different values of the cutoff $\Lambda_1 < \Lambda_2 < \Lambda_3$, in arbitrary units. The plot is qualitative, but shows clearly that with a regulated noise, only the short-distance behaviour is affected.

Generally speaking, the stationary distribution probability of the regulated stochastic process is given by [19]

$$\mathcal{P}_\Lambda(\phi) = \frac{1}{Z} \exp\left(-S_\Lambda[\phi]\right) = \frac{1}{Z} \exp\left(-(S[\phi] + \Delta S_\Lambda[\phi])\right), \qquad (2.13)$$

where the correction term $\Delta S_\Lambda[\phi]$, reads, for a regulator $r_\Lambda(p^2)$,

$$\Delta S_\Lambda[\phi] = \frac{1}{2} \int_p \phi_p \, \Lambda^2 \left(\frac{1}{r_\Lambda(p^2)} - 1\right) \phi_{-p}.$$

at this point mention that this is the stationary pdf that one gets with frg for sharp cutoff, and cite some papers.

2.4 Chiral symmetry

In this section we want to introduce chiral symmetry and its breaking, both in the continuum and on the lattice.
It is useful to adopt the notation

$$\psi = (\psi^{(1)}, \ldots, \psi^{(N_f)}).$$

We then introduce left-handed and right-handed spinors

$$\psi_L = (1 - \gamma_5)\,\psi, \qquad \psi_R = (1 + \gamma_5)\,\psi,$$

for which

$$\psi = \frac{(1 - \gamma_5)}{2}\psi + \frac{(1 + \gamma_5)}{2}\psi = \psi_L + \psi_R.$$

2.4.1   Chiral symmetry in the continuum

The free massless Dirac Lagrangian

$$\mathcal{L}_D = \bar{\psi}\slashed{\partial}\psi = \bar{\psi}_L\slashed{\partial}\psi_L + \bar{\psi}_R\slashed{\partial}\psi_R \tag{2.14}$$

is symmetric under the chiral group $SU(N_f)_L \times SU(N_f)_R$, namely

$$\psi_L(x) \to U_L\psi_L(x), \qquad \bar{\psi}_L(x) \to \bar{\psi}_L(x)U_L^\dagger,$$
$$\psi_R(x) \to U_R\psi_R(x), \qquad \bar{\psi}_R(x) \to \bar{\psi}_R(x)U_R^\dagger,$$

for $U_L, U_R \in SU(N_f)$.
In terms of the full spinor ψ, the chiral symmetry can be written as

$$\psi \to M\,\psi, \qquad \bar{\psi} \to \bar{\psi},$$

where

$$M = e^{i(\theta_a\tau^a + \gamma_5\beta_a\tau^a)}, \quad \tau^a \in su(N_f)$$

so that

$$SU(N_f)_L \times SU(N_f)_R \simeq SU(N_f)_V \times SU(N_f)_A.$$

$SU(N_f)_V$ is the isospin subgroup, characterised by $\beta_a = 0$, and $SU(N_f)_A$ is the axial rotation subgroup, characterised by $\theta_a = 0$.
To be more precise, the full invariance group of the classical action is

$$SU(N_f)_L \times SU(N_f)_R \times U(1)_A \times U(1)_V,$$

where the axial and vector symmetry transformations are, respectively,

$$\psi \to e^{i\theta\gamma_5}\,\psi, \qquad \psi \to e^{i\theta}\,\psi.$$

One can thus prove that axial symmetry is broken by quantum anomalies (see for example [20]), so that the symmetry in the quantum case is

$$SU(N_f)_L \times SU(N_f)_R \times U(1)_V.$$

If equal masses for each flavour are introduced, then the symmetry group reduces to the isospin subgroup, diagonal in flavour space

$$SU(N_f)_V \times U(1)_V.$$

Finally, if the fermions have different masses, the symmetry group reduces to

$$\underbrace{U(1) \times \cdots \times U(1)}_{N_f} \times U(1)_V.$$

2.4.2   Chiral symmetry on the lattice

The essence of chiral symmetry for fermions can be expressed as [21]

$$\{\gamma_5, D\} = 0 \tag{2.15}$$

Implementing chiral symmetry on a finite-volume spacetime lattice, is a hard task. This is because, as proven by Nielsen and Ninomiya, one either has chiral symmetry

on the lattice, or solves the doubling problem citationsssss.

In particular, the insertion of the Wilson term in the action, as shown in Appendix B, causes explicit breaking of the chiral symmetry. If one's goal is to study spontaneous symmetry breaking, this constitues a problem. Thus, many options have been proposed to circumvent the issue. As an example we mention the approach by Ginsparg and Wilson citationsssss, who proposed to modify the chiral symmetry condition (2.4) to

$$\{\gamma_5, D\} = a\, D\gamma_5 D$$

The right hand-side of the equation vanishes in the continuum limit $a \to 0$. In this way, one can define chiral symmetry on the lattice remaining consistent in the continuum limit. This approach will not be pursued further and we ask the reader to consult appropriate references [13, 21] for a detailed treatment.

Our approach to study chiral symmetry will be discussed and motivated in section 4.4.

2.5 Yukawa theory

2.5.1 Description of the model

Let us consider the Yukawa theory defined by the action

$$
\begin{aligned}
S[\phi, \psi, \bar{\psi}] &= S_\phi[\phi] + S_\psi[\psi, \bar{\psi}] + S_{\text{int}}[\phi, \psi, \bar{\psi}], \\
S_\phi[\phi] &= \int_x \phi_x \left(-\frac{\partial_x^2}{2} + \frac{m_\phi^2}{2} \right) \phi_x + \frac{\lambda}{4!}\, \phi_x^4, \\
S_\psi[\psi, \bar{\psi}] &= \int_x \sum_{f=1}^{N_f} \bar{\psi}_x^{(f)} \left(\slashed{\partial}_x + m_q \right) \psi_x^{(f)}, \\
S_{\text{int}}[\phi, \psi, \bar{\psi}] &= \int_x \sum_{f=1}^{N_f} g\, \bar{\psi}_x^{(f)}\, \phi_x\, \psi_x^{(f)}.
\end{aligned}
\tag{2.16}
$$

One can see that the action is made of a scalar part $S_\phi[\phi]$, a fermionic part $S_\psi[\psi, \bar{\psi}]$ and a Yukawa interaction term $S_{\text{int}}[\phi, \psi, \bar{\psi}]$.

In pratice we will work with fixed number of flavours $N_f = 2$, but it is useful to keep track of N_f and set it to its value when needed.

It is also convenient for later purposes to define the operators K, D represented in position space as

$$
\begin{aligned}
K(x, y) &= \left(-\partial_x^2 + m_\phi^2 \right) \delta(x, y), \\
D(x, y) &= \left(\slashed{\partial}_x + m_q + g\phi \right) \delta(x, y),
\end{aligned}
\tag{2.17}
$$

and in momentum space as

$$
\begin{aligned}
\widetilde{K}(p, q) &= \int_{x,y} e^{-ipx} \left(\partial_x^2 + m_\phi^2 \right) \delta(x, y)\, e^{iqy} = \left(\frac{p^2}{2} + \frac{m_\phi^2}{2} \right) \delta(p, q), \\
\widetilde{D}(p, q) &= \int_{x,y} e^{-ipx} \left(\slashed{\partial}_x + m_q + g\phi \right) \delta(x, y)\, e^{iqy} = \left(\slashed{p}_x + m_q + g\phi \right) \delta(p, q).
\end{aligned}
\tag{2.18}
$$

This allows one to rewrite the action as

$$S[\phi, \psi, \bar{\psi}] = \int_x \frac{1}{2} \phi_x K_{xx} \phi_x + \frac{\lambda}{4!} \phi_x^4 + \sum_{f=1}^{N_f} \bar{\psi}_x^{(f)} D_{xx} \psi_x^{(f)}.$$

2.5.2 Chiral symmetry in the Yukawa model

The action written in terms of ψ_L, ψ_R, reads

$$S = S_\phi + \int_x \left[\bar{\psi}_L D \psi_L + \bar{\psi}_R D \psi_R + (m_q + g\phi) \left(\bar{\psi}_L \psi_R + \bar{\psi}_R \psi_L \right) \right]. \tag{2.19}$$

The action is not invariant under the full chiral group, but if $m_q = 0$ it is symmetric under the discrete chiral transformation

$$\phi \to -\phi,$$
$$\psi_L \to \gamma_5 \psi_L, \qquad \bar{\psi}_L \to \bar{\psi}_L \gamma_5,$$
$$\psi_R \to \gamma_5 \psi_R, \qquad \bar{\psi}_R \to \bar{\psi}_R \gamma_5,$$

typical of theories such as the Gross-Neveu model citationsssss. In order to generalise the model to the full chiral group, one has to consider an $O(4)$ scalar sector and interactions, since $O(4) \simeq SU(2) \times SU(2)$. Similar effective theories with such properties are, for example, the Nambu-Jona-Lasinio model and the Quark-Meson model citationssssss. Thus, since we are in $1+1$ dimensions, spontaneous breaking of continuous symmetries is forbidden by the Mermin-Wagner theorem citationsssss, and we decided to opt for a simple Yukawa theory.

We now want to discuss more in detail the phenomenom of (discrete) chiral symmetry breaking and how it can happen in the model. In fact, the latter can happen either explicitly in the classical action, if a finite quark mass is added, or spontaneously, if $\langle \phi \rangle \neq 0$.
To better see this, let us perform the fermionic path integral explicitly

$$\int \mathcal{D}\bar{\psi}\mathcal{D}\psi \, \exp\left(-\int_x \sum_{f=1}^{N_f} \bar{\psi}_x^{(f)} D \psi_x^{(f)} \right) = (\det D[\phi])^{N_f} = e^{N_f \, \text{Tr} \log(D[\phi])},$$

where the trace is performed over spacetime and spinor components.
The full path integral can now be expressed in terms of the resulting effective action for the scalar fields

$$Z = \int \mathcal{D}\phi \, e^{-S_{\text{eff}}[\phi]},$$

with

$$S_{\text{eff}}[\phi] = S_\phi[\phi] - N_f \, \underset{x,s}{\text{Tr}} \, \log D[\phi]. \tag{2.20}$$

One can derive the classical equations of motion by imposing $\frac{\delta S}{\delta \phi} = 0$, here expressed in momentum space

$$(k^2 + m_\phi^2) \, \phi(x) + \frac{\lambda}{6} \phi^3(x) = N_f g \, \underset{s}{\text{Tr}} \left[D^{-1}(\phi(x)) \right] = -N_f g \, \bar{\psi}(x)\psi(x) \tag{2.21}$$
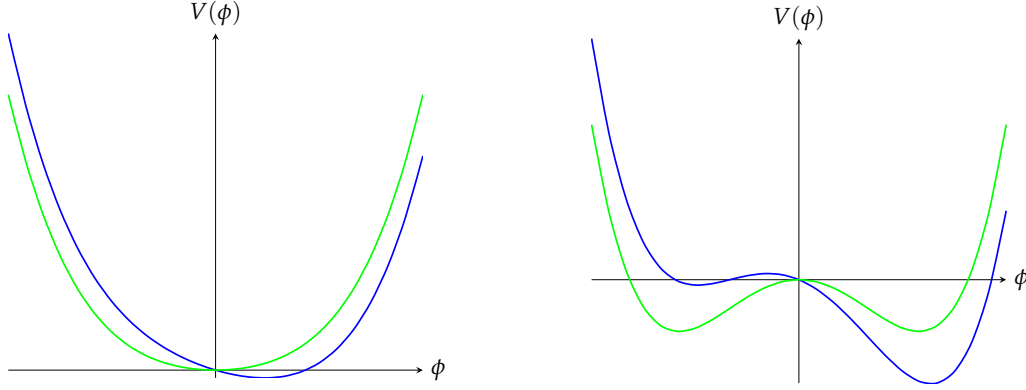
FIGURE 2.3: The introduction of the boson-fermion interaction, with a finite fermionic mass, causes explicit breaking of chiral symmetry, with consequence spontaneous breaking of the O(1) symmetry according to (2.23). It shifts the equilibrium position in the symmetric phase (left) causing $\langle \phi \rangle \neq 0$, and tilts the potential in the broken phase (right), making the two minima not equivalent.

For $\lambda = 0$, they highlight a simple proportionality relation between magnetisation and chiral condensate, which reads

$$\phi = -\frac{N_f \, g}{k^2 + m_\phi^2} \, \bar{\psi}\psi. \tag{2.22}$$

This relation, which was here derived at the classical level, is proven to hold also in mean field on the quantum level [22] and makes apparent the role of ϕ as a quark bilinear.

When bosons self-interactions are added, namely when $\lambda \neq 0$, the full relation between ϕ and the chiral condensate $\bar{\psi}\psi$ is given by (2.22), but still one expects, qualitatively,

$$\langle \phi \rangle \sim \langle \bar{\psi}\psi \rangle. \tag{2.23}$$

A non-vanishing condensate is also related to a physical quark mass [22, 23], while the presence of magnetisation causes the breaking of $O(1)$ symmetry. If $\langle \phi \rangle = v$, one can write $\phi(x) = v + \varphi(x)$ and the massless lagrangian assumes the form

$$S = S_\phi + \int_x [\bar{\psi}_L \, D \, \psi_L + \bar{\psi}_R \, D \, \psi_R + gv \, (\bar{\psi}_L \psi_R + \bar{\psi}_R \psi_L)] + g\varphi(x) \, (\bar{\psi}_L \psi_R + \bar{\psi}_R \psi_L)$$

hence showing that one can expect

$$\langle \phi \rangle \sim \langle \bar{\psi}\psi \rangle \sim m_q. \tag{2.24}$$

2.5.3 Phase structure and order parameters

We want to conclude this chapter by commenting on the phase strcture of the Yukawa theory. This will guide the choice of parameters for the investigation carried in the remaining sections. A sketch of the different phases of the model is reported in figure 2.4. The order parameters are the magnetisation $M = \langle \phi \rangle$ and the staggered
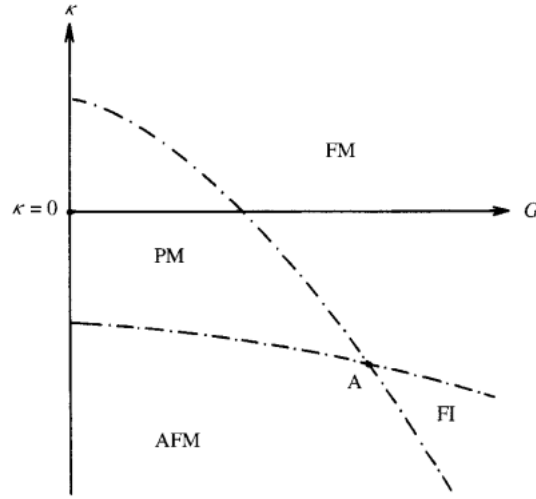
FIGURE 2.4: General phase diagram of a Yukawa theory.
I know that I wouldn't be allowed to use this picture, I will see later
what to do.

magnetisation $M_s = \langle \Phi \rangle$, where

$$\Phi_x \equiv (-1)^{t+x} \phi_x = \mathrm{e}^{\mathrm{i}\pi(t+x)} \phi_x. \tag{2.25}$$

The four different phases are characterised by the following combinations of the order parameters

- paramagnetic phase: $M = 0, M_s = 0$,

- ferromagnetic phase: $M \neq 0, M_s = 0$,

- anti-ferromagnetic phase: $M = 0, M_s \neq 0$,

- ferrimagnetic phase: $M \neq 0, M_s \neq 0$.

The lattice observables used for the investigation are introduced in section 3.4.

Chapter 3

Methods and algorithms

3.1 Discretisation of the Yukawa theory

In order to make the theory suitable for a numerical simulation on a computer, the continuum formulation of the Yukawa model, which has been introduced in section 2.5, has to be discretised. Here we provided a sketch of a discretisation procedure, and we refer to other resources [13, 21, 24, 25] for further details.

For what concerns the bosonic part of the action, a discretisation can be done straightforwardly with the following replacements

$$\int d^x \quad \rightarrow \quad a^2 \sum_x,$$

$$\partial_t^2 + \partial_x^2 = \frac{\partial^2}{\partial t^2} + \frac{\partial^2}{\partial x_1^2} \quad \rightarrow \quad \sum_\mu \left[\frac{\delta_{m,n+\mu} + \delta_{m,n-\mu} - 2\delta_{m,n}}{a^2} \right],$$

which yields to the lattice action

$$S_\phi[\phi] = a^2 \left(\frac{1}{2} \sum_{m,n} \phi_m \, K_{mn} \, \phi_n + \frac{\lambda}{4!} \sum_n \phi_n^4 \right)$$

$$= \frac{1}{2} \sum_{m,n} \hat{\phi}_m \, \widehat{K}_{mn} \, \hat{\phi}_n + \frac{\hat{\lambda}}{4!} \sum_n \hat{\phi}_n^4,$$

where we expressed everything in dimensionless quantities

$$\hat{m}_\phi^2 = a^2 \, m_\phi^2,$$
$$\hat{\lambda} = a^2 \, \lambda, \tag{3.1}$$
$$\widehat{K}_{mn} = a^2 K_{mn}.$$

The operator components $\widehat{K}_{mn}$ are the discretised version of (2.17)

$$\widehat{K}_{mn} = -\sum_\mu \left[\delta_{m,n+\mu} + \delta_{m,n-\mu} - 2\,\delta_{m,n} \right] + \hat{m}_\phi^2 \, \delta_{mn} \tag{3.2}$$

and its representation in momentum space is

$$
\begin{aligned}
\widehat{K}_{p,q} &= \sum_{n,m} e^{ipn}\, \widehat{K}_{nm}\, e^{-iqm} \\
&= \sum_{n,m} e^{ipn} \left(-\sum_\mu \left[\delta_{m,m+\mu} + \delta_{m,m-\mu} - 2\delta_{m,n} \right] + \hat{m}_\phi^2\, \delta_{mn} \right) e^{-iqm} \\
&= \sum_n e^{i(p-q)n} \left[\hat{m}_\phi^2 + 2\sum_\mu \left(1 - \cos\left(q_\mu \right) \right) \right] \\
&= \left[\hat{m}_\phi^2 + \sum_\mu 4\sin^2\left(\frac{p_\mu}{2} \right) \right] \delta(p-q).
\end{aligned}
$$

For what concerns the fermionic action, a naïve discretisation is not sufficient, due to the well known doubling problem [13, 25]. In this work Wilson fermions [26] are employed as a way to fix such issue. Details of this formulation are explained in Appendix B. Here, only the final discretised action is reported, which reads

$$
S_\psi\left[\hat{\psi}, \hat{\bar{\psi}} \right] + S_{\text{int}}\left[\hat{\phi}, \hat{\psi}, \hat{\bar{\psi}} \right] = \sum_{f=1}^{N_f} \hat{\bar{\psi}}_m^{(f)}\, \widehat{D}_{mn}\, \hat{\psi}_n^{(f)}, \tag{3.3}
$$

with ψ_n beeing a two-component spinor, and $\widehat{D}_{m,n}$ the Wilson-Dirac operator defined as

$$
\begin{aligned}
\widehat{D}_{m,n} = &-\left(\frac{\Gamma_{+\hat{0}}}{2}\, \delta_{m,m+\hat{0}} + \frac{\Gamma_{-\hat{0}}}{2}\, \delta_{m,m-\hat{0}} + \frac{\Gamma_{+\hat{1}}}{2}\, \delta_{m,m+\hat{1}} + \frac{\Gamma_{-\hat{1}}}{2}\, \delta_{m,m-\hat{1}} \right) \\
&+ (2ar + \hat{m} + \hat{g}\phi)\, \delta_{s,s'}\, \delta_{m,n}.
\end{aligned} \tag{3.4}
$$

Note that the interaction term $g\,\bar{\psi}\phi\psi$ has been included in the definition of D. The Wilson projectors $\Gamma_{\pm\hat{\mu}}$ are defined as

$$
\Gamma_{\pm\hat{\mu}} = ar\,\mathbb{1}_s \mp \gamma_\mu.
$$

Since $r \in [0,1]$ is a free parameter, in this work we set $r = 1$, if not otherwise specified.

In summary the discretised action for the Yukawa model is

$$
S\left[\hat{\phi}, \hat{\psi}, \hat{\bar{\psi}} \right] = \sum_{m,n} \hat{\phi}_m\, \widehat{K}_{m,n}\, \hat{\phi}_n + \frac{\hat{\lambda}}{4!}\, \hat{\phi}_m^4\, \delta_{m,n} + \sum_{f=1}^{N_f} \hat{\bar{\psi}}_m^{(f)}\, \widehat{D}_{mn}\hat{\psi}_n^{(f)}, \tag{3.5}
$$

with $\widehat{K}_{mn}$, $\widehat{D}_{mn}$ given respectively by (3.2) and (3.4).

For later reference, we also report the discretised version of the effective action (2.20)

$$
\begin{aligned}
S_{\text{eff}}[\hat{\phi}] &= S_\phi[\hat{\phi}] - N_f \underset{n,s}{\text{Tr}} \log \widehat{D} \\
&= \sum_{m,n} \hat{\phi}_m\, \widehat{K}_{m,n}\, \hat{\phi}_n + \frac{\hat{\lambda}}{4!}\, \hat{\phi}_m^4\, \delta_{m,n} - N_f \underset{n,s}{\text{Tr}} \log \widehat{D}_{nn}.
\end{aligned} \tag{3.6}
$$

The full discrete path-integral reads

$$
Z = \int \prod_n d\hat{\phi}_n\, e^{-S_{\text{eff}}[\hat{\phi}]}. \tag{3.7}
$$

In the remaining of this work, both the original action S and the effective action S_{eff} will be denoted by S for simplicity. It will be clear from the context which of the two we will be referring to.

3.2 Langevin Monte Carlo

The relations (**??**) suggest that equation (2.6) can be integrated numerically for discrete time steps τ_n to generate field configurations distributed according to (2.9). The simplest first-order integration algorithm is the Euler-Majorana scheme [16]

$$\phi(\tau_{n+1}, x) = \phi(\tau_n, x) - \epsilon \frac{\delta S[\phi]}{\delta \phi(\tau_n, x)} + \sqrt{\epsilon}\, \eta(\tau_n, x) + O(\epsilon^2),$$

where $\epsilon = \tau_{n+1} - \tau_n$. Higher order integration schemes are possible (see e.g.[27, 28]), but not adopted in this work, and an adaptive step size is employed as detailed in Appendix C. In this way, for any observable O, one can introduce a Monte-Carlo estimator $\langle O \rangle_*$ which converges to the expectiation value given by (2.10) in the limit of infinite samples

$$\langle O \rangle_* = \frac{1}{N_{\text{samp}}} \sum_{i=1}^{N_{\text{samp}}} O_i \xrightarrow[N_{\text{samp}} \to \infty]{} \langle O \rangle = \frac{1}{Z} \int D\phi\, O(\phi) \exp\left(-S[\phi]\right), \qquad (3.8)$$

where $O_i = O(\phi(\tau_i))$ is the sample of the observable O done at time τ_i.

For the discretised action of the Yukawa theory (3.6) the drift reads, explicitly,

$$\begin{aligned}
\frac{\partial S}{\partial \hat{\phi}_m(\tau_n)} &= \frac{\partial S_{\hat{\phi}}}{\partial \hat{\phi}_m(\tau_n)} - N_f \operatorname*{Tr}_s \left[\sum_{j,k} \widehat{D}_{jk}^{-1} \frac{\partial \widehat{D}_{kj}(\hat{\phi})}{\partial \hat{\phi}_m(\tau_n)} \right] \\
&= \sum_l \widehat{K}_{ml}\, \hat{\phi}_l + \frac{\hat{\lambda}}{6}\, \hat{\phi}_m^3 - \hat{g}\, N_f \operatorname*{Tr}_s \left[(\widehat{D}_{mm})^{-1}(\hat{\phi}(\tau_n)) \right].
\end{aligned} \qquad (3.9)$$

While the bosonic contribution can be computed in a straightforward manner, the computation of the fermionc contribution requires the inversion of the Dirac operator. This, in general, cannot be done straightforwardly, mainly due to computational reasons. In fact, the full Dirac operator would be a $(2 \cdot N_t \cdot N_x \cdot N_f)^2$ dimensional object and a full inversion would be very expensive. In fact, D^{-1} has to be recomputed at every step and the best available algorithm as today for the matrix inversion has a computational complexity of $O(n^{2.371552})$ [29]. To circumvent this, we use the bilinear noise scheme [27, 30] which is illustrated in Appendix C.

3.3   Applications of coloured noise in lattice QFT

After the general introduction on coloured noise given in the previous paragraph, let us now look more closely on the lattice formulation and at some possible applications of the technique, some of which will be studied numerically in chapter 4.

To this end, let us consider a two-dimensional lattice with side lengths L_t, L_x and spacing $a = a_x = a_t$. This implies a maximum momentum $p_{max} = \pi/a$ in each spacetime direction and $N_x = L_x/a, N_t = L_t/a$ points in each direction. Let us also define

$$\Lambda_0^2 \equiv (p_{max}^x)^2 + (p_{max}^t)^2, \tag{3.10}$$

which indicates the maximum squared momentum on the given lattice.
We then consider a simulation with a regularised noise defined by a cutoff $\Lambda \leq \Lambda_0$ and we define a dimensionless parameter

$$s^2 = \frac{\Lambda^2}{\Lambda_0^2}, \qquad 0 \leq s \leq 1. \tag{3.11}$$

Note that Λ implicitly defines a length scale given by $a_{eff} = \pi/\Lambda$.

3.3.1   Classical to quantum interpolation

The use of coloured noise, allows for a smooth interpolation between the fully classical and fully quantum picture. In fact, one can perform various simulations changing the value of the cutoff fraction s and adding or removing quantum degrees of freedom, as pictured in figure add figure. This can be used either to investigate the role of quantum fluctuations in the system, or to remove irrelevant degrees of freedom, resulting in a speed-up of the simulation.

3.3.2   Noise-induced transition

Noise-induced transition is a well known field of stochastic dynamics [18, 31, 32] and consists in investigating whether noise can qualitatively affect the behaviour of a system. In our case, since noise is due to quantum fluctuations, we are interested in understanding if quantum fluctuations can trigger a phase transition with respect to the classical system, with the same parameters settings.
This question will be addressed in section 4.4 and it will be shown that for small negative bosonic mass, the classical system lies in a state of broken symmetry, while in the quantum case, the symmetry is restored.

3.3.3   Cooling and the continuum limit of effective theories

Following the paradigm of Kadanoff-Wilson of chapter 2, we want to use RG properties to encode quantum fluctuations in a redefinition of the couplings of the bare action. This removes short-distance fluctuations from the simulation, without changing the physical content of the theory. Note that this would, in principle, require a detailed knowledge of the β-functions of the theory. Thus, for sufficiently high cutoff, approximate Ansatz such as dimensional rescalings are generally enough. We will pursue this way, as follows.

Let us consider a simulation with $s = 1$ and a set of bare couplings $\{g_0^i\}$, and another simulation with $s' < 1$ and new set of couplings $\{g_0^{i\prime}\}$.

For what concerns the scalar part of the action, a dimensional rescaling, which corresponds to a tree-level RG transformation, is rather straightforward

$$\hat{m}_\phi^2 = (a^2 m_\phi^2) \;\rightarrow\; s^2(a^2 m_\phi^2) = s^2\,\hat{m}_\phi^2, \qquad \hat{\lambda} = (a^2\lambda) \;\rightarrow\; s^2(a^2\lambda) = s^2\hat{\lambda},$$
$$\hat{\phi} = \phi \;\rightarrow\; \phi = \hat{\phi}.$$

The fermionic part needs some more careful analysis. For simplicity, let us for the moment set $N_f = 1$.

In a lattice simulation one wants to perform the integral over the fermionic fields and works with the effective action (2.20). In this case the drift is given by equation (3.9), with the fermionic contribution

$$K_\psi = g \operatorname*{Tr}_s D^{-1}, \tag{3.12}$$

or, in terms of dimensionless quantities,

$$\widehat{K}_\psi = (ag) \operatorname*{Tr}_s (aD)^{-1}.$$

This implies that under a lattice block-spin transformation, where $a \rightarrow sa$,

$$\widehat{K}_\psi \rightarrow (sag) \operatorname*{Tr}_s (saD)^{-1} = \widehat{K}_\psi. \tag{3.13}$$

On the other side, when computing the drift via the original action (2.16), one gets

$$K = -\frac{\delta S}{\delta\phi} = K_\phi - g\,\bar{\psi}\psi =$$
$$= -\hat{K}_{mn}\,\phi_n - \frac{\lambda}{6}\,\phi^3 - g\,\bar{\psi}\psi. \tag{3.14}$$

where, in the last row, $\widehat{K}_{mn}$ indicates the bosonic operator components (3.2).

The fermionic contribution is given by

$$K'_\psi = -g\,\bar{\psi}\psi.$$

Note that all the terms in the equation (3.14) have dimension 2, in units of energy, which means, in particular, that after a lattice block-spin transformation where $a \rightarrow sa$, one has

$$\widehat{K}'_\psi = (ag)(a\bar{\psi}\psi) \rightarrow s^2(ag)(a\bar{\psi}\psi) = s^2\widehat{K}'_\psi, \tag{3.15}$$

in contrast with (3.13). For this reason, in order to have the correct scaling, we compute the contribution to the drift without rescaling the Dirac operator (and hence the Yukawa coupling), and then rescale the whole drift via

$$\widehat{K}_\psi \rightarrow s^2\widehat{K}_\psi,$$

so that the scaling dimension of the other terms in (3.14) is matched.

We want to mention that the cooling procedure has important consequences on the issue of continuum limit of low-energy effective theories. In fact, in the standard lattice regularisation procedure, one always has $a \sim \Lambda_0^{-1}$, which means that the continuum limit $a \rightarrow 0$ is always connected to the limit $\Lambda_0 \rightarrow \infty$, in accordance to what

discussed in sections 2.1 and 2.2.

3.3.4   Control over temperature

there will be no simulations regarding this. should I write it anyway? I think it is important.

3.4   Definition of relevant observables

We define the magnetisation M of the field ϕ as

$$M = \left\langle \frac{1}{V} \sum_n \phi_n \right\rangle.$$

Thus, in a finite volume lattice system, the absolute magnetisation

$$M = \left\langle \frac{1}{V} \left| \sum_n \phi_n \right| \right\rangle.$$

is better suited as an order parameter [15, 21].
In the continumm, phase transition is characterised by a divergence in the susceptibility, or connected two-points function

$$\chi_2 = V \left(\langle M^2 \rangle - \langle M \rangle^2 \right) = V \left\langle (M - \langle M \rangle)^2 \right\rangle.$$

On a finite volume lattice, one obseres a peak that becomes sharper as the volume is increased. In pratice, the susceptibility of the order parameter

$$\chi_2 = V \left\langle (M - \langle |M| \rangle)^2 \right\rangle$$

will be adopted.
We define the fermionic two-points function

$$
\begin{aligned}
\langle \psi_m \bar{\psi}_n \rangle &= \frac{1}{Z} \int \mathcal{D}\phi \, \mathcal{D}\psi \, \mathcal{D}\bar{\psi} \, \psi(x) \, \bar{\psi}(y) \, \exp\left(-S_\phi - \psi D \psi + \bar{\eta}\psi + \bar{\psi}\eta \right) \\
&= \frac{1}{Z} \int \mathcal{D}\phi \, \mathcal{D}\psi \, \mathcal{D}\bar{\psi} \, \frac{\delta}{\delta\bar{\eta}_m} \frac{\delta}{\delta\eta_n} \exp\left(-S_\phi - \psi D \psi + \bar{\eta}\psi + \bar{\psi}\eta \right) \\
&= \frac{1}{Z} \int \mathcal{D}\phi \, \det[D(\phi)] \, \exp\left(-S_\phi \right) \, \frac{\delta}{\delta\bar{\eta}_m} \frac{\delta}{\delta\eta_n} \exp\left(\bar{\eta} D^{-1} \eta \right) \\
&= \left\langle \left[D^{-1}(\phi) \right]_{mn} \right\rangle.
\end{aligned}
\tag{3.16}
$$

where D is the the Wilson-Dirac operator.
From this, the chiral condensate follows straightforwardly

$$\langle \bar{\psi}\psi \rangle = \sum_{n,s} \langle \bar{\psi}_{n,s} \, \psi_{n,s} \rangle = -\underset{n,s}{\mathrm{Tr}} \, (D^{-1})_{nn}.$$

The fermionic correlator is defined as

$$C_\psi(t,0) \equiv \frac{1}{N_x} \sum_{n_x} \left[\langle \psi(t,n_x) \, \bar{\psi}(0,0) \rangle - \langle \psi(N_t - t, n_x) \, \bar{\psi}(0,0) \rangle \right].$$

Note that we sum up two waves because the source propagates both forward and backward in time due to the boundary conditions.

As shown in Appendix A (not yet), for $t \to \infty$ one has

$$C_\psi(t, 0) \approx \sinh\left(E_0^\psi \left(\frac{N_t}{2} - t \right) \right),$$

where E_0^ψ is the fermionic mass gap, which will be denoted as $m_{q,\text{phys}}$.

Analogously, the bosonic correlator is

$$C_\phi(t, 0) \equiv \frac{1}{N_x} \sum_{n_x} \left[\langle \phi(t, n_x) \, \phi(0, 0) \rangle + \langle \phi(N_t - t, n_x) \, \bar{\phi}(0, 0)] \rangle \right.$$

and for $t \to \infty$ one has

$$C_\phi(t, 0) \approx \cosh\left(E_0^\phi \left(\frac{N_t}{2} - t \right) \right).$$

$E_0^\phi \equiv m_{\phi,\text{phys}}$ is the bosonic mass gap.

Chapter 4

Numerical investigation

4.1 The fermionic correlator

To start with the study of the model, we want to analyse the behaviour of the fermionic correlator and illustrate the fermionic masses extraction procedure.
Let us initially restrict to $g = 0$, so that add wilson

$$D_{nm} = \sum_{\hat{\mu}} \left[\frac{\gamma_{\hat{\mu}} \delta_{n+\hat{\mu},m} - \gamma_{\hat{\mu}} \delta_{n-\hat{\mu},m}}{2} + m_q \, \delta_{nm} \right].$$

In this case, an analytical expression of the fermionic mass can be derived as follows. The Dirac operator in momentum space reads

$$\bar{D}(p) = m_q + \sum_{\mu} 2 \sin^2 \left(\frac{p_{\mu}}{2} \right) + i \sum_{\mu} \gamma_{\mu} \sin \left(p_{\mu} \right)$$

The inverse can be checked to be

$$\bar{D}^{-1}(p) = \frac{m_q + \sum_{\mu} 2 \sin^2 \left(\frac{p_{\mu}}{2} \right) - i \sum_{\mu} \gamma_{\mu} \sin \left(p_{\mu} \right)}{\left[m_q + \sum_{\mu} 2 \sin^2 \left(\frac{p_{\mu}}{2} \right) \right]^2 + \left[\sum_{\mu} \gamma_{\mu} \sin \left(p_{\mu} \right) \right]^2}$$

One can now find the pole mass by imposing

$$\left[m_q + \sum_{\mu} 2 \sin^2 \left(\frac{p_{\mu}}{2} \right) \right]^2 \Bigg|_{p_{\mu} = (im_{\text{phys}}, 0)} + \left[\sum_{\mu} \gamma_{\mu} \sin \left(p_{\mu} \right) \right]^2 \Bigg|_{p_{\mu} = (im_{\text{phys}}, 0)} = 0$$

This results in a trascendental equation

$$\left[m_q - 2 \sinh^2 \left(\frac{m_{\text{phys}}}{2} \right) \right]^2 - \sinh^2 \left(m_{\text{phys}} \right) = 0$$

This equation has the solution

$$m_{\text{phys}} = \log \left(1 + m_q \right)$$

We then compute the correlator numerically via a single inversion of the Dirac operator as detailed in Appendix C. The lattice volume is chosen to be 128×128. Figure 4.1 reports the fermionic correlator as a function of m_q. One can see that a big bare quark mass results in a quick decay, while a small mass tends to deform the characteristic shape of the correlator.
Figure 4.2 shows the number of iterations needed for convergence. While the exact
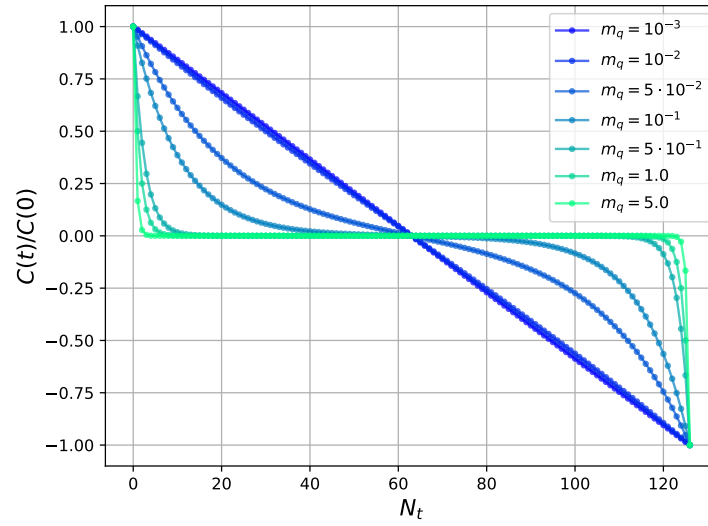
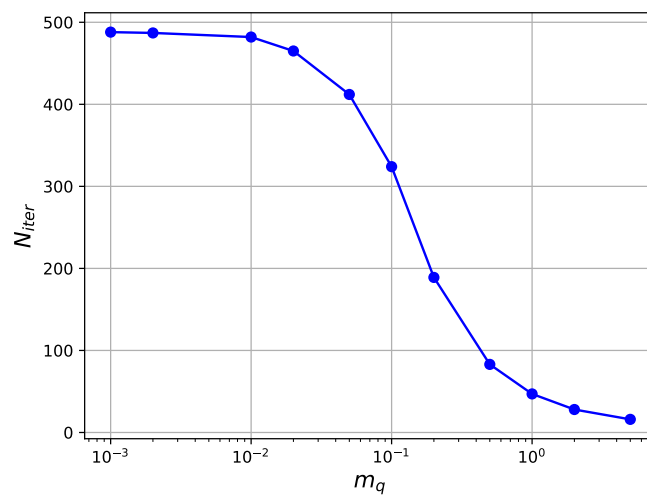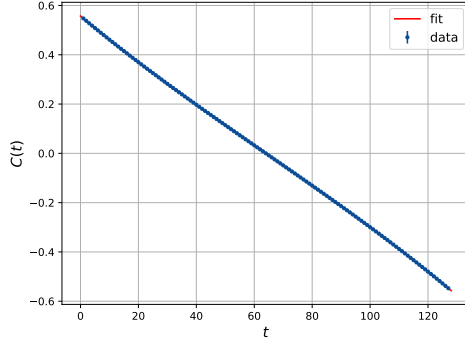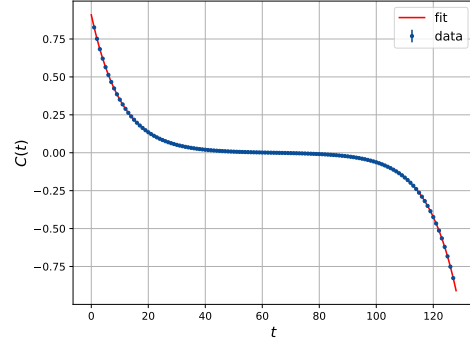FIGURE 4.1: Correlator as a function of the bare mass
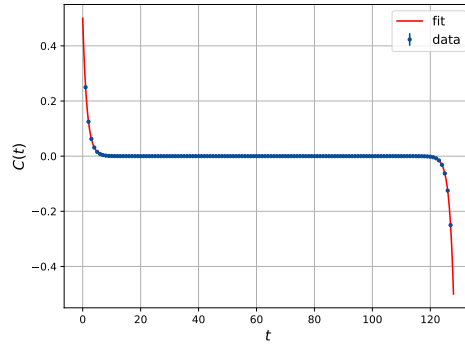

FIGURE 4.2: CG iterations

m_q	teo	fit	err
1.0	0	0.6931537171644739	4e-20
0.1	0	0.09531020915059212	0.004
0.01	0	0.009950277657505842	0.8

(A) Caption for Image 1

(B) Caption for Image 2

(C) Caption for Image 3

FIGURE 4.3: Overall Caption for the Figure

number depends on the desired tolerance, one can clearly see that the number of iterations grows as $m_q \rightarrow 0$ due to an increase in the condition number [33]. does the condition number increase even more for naive fermions?
We then choose three values of the bare quark mass and perform a fit according to (**??**), in order to extract the physical mass and we compare it to the theoretical value given by add ref. eq.. The results are reported in figures **??** and table **??**.

The presence of a background field has the same effects on the correlator as a bare quark mass. In fact, if $\phi(x) = v$, one can simply redefine the bare mass as $M_q = m_q + g\,v$ and the properties of the fermionic correlator remain unchanged.

<div align="center">
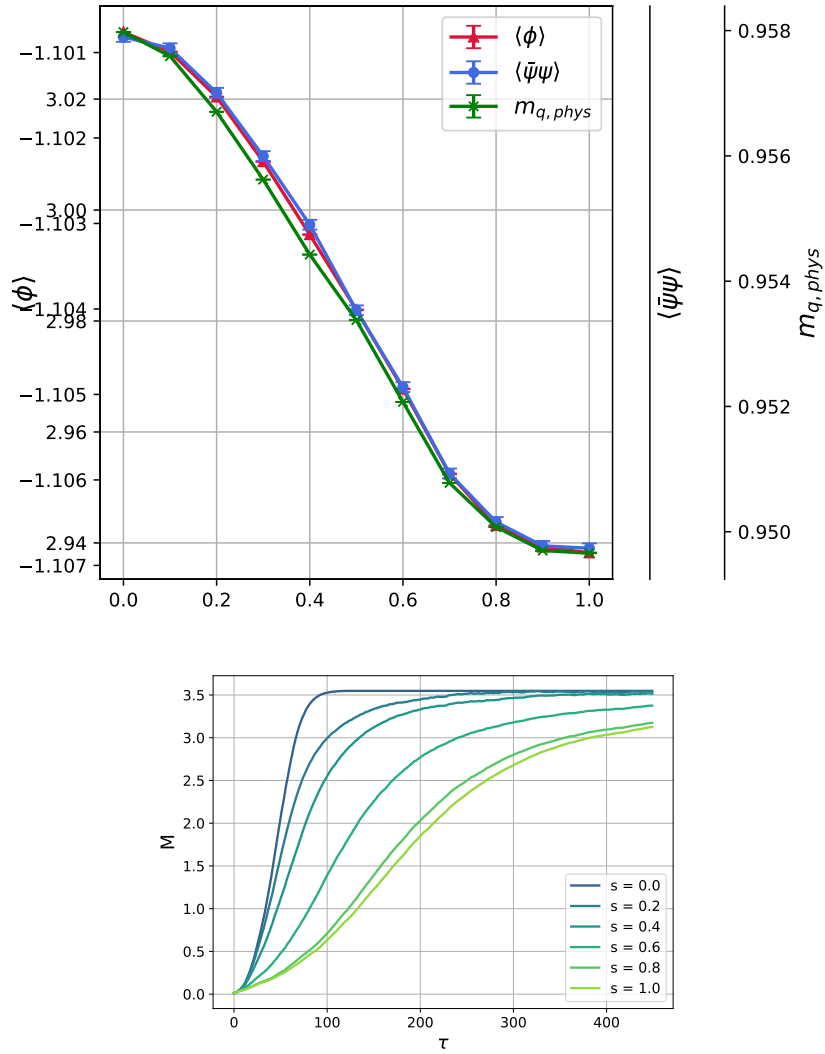
FIGURE 4.4

</div>

4.2   Classical-to-quantum interpolation

Let us start by analising the coloured noise field in the simulation and relevant properties that emerge from it. We consider the Yukawa model described by the continuum action (2.16) and its discrete vesion (3.5), (3.6).

Figure 4.4 reports the Langevin evolution of the system for different noise fractions. The red line corresponds to the case $s = 0$, namely a classical simulation, while the blue line corresponds to the case $s = 1$, namely the fully quantum case. Note that a lower noise fraction is correlated to a faster convergence towards equilibrium. Moreover, low-distance fluctuations are suppressed due to the removal of the ultraviolet modes in the noise term.

We now move on to analyse equilibrium properties. Coloured noise allows for a smooth interpolation between the fully quantum and fully classical picture, with a consequent shift of the expectation values of the observables. Figures **??**,**??** report, respectively, the magnetisation and the chiral condensate as a function of the noise fraction s. All the quntities in the classical action, including the coupling constants,

are kept fixed while changing s. Each figure reports two plots corresponding to two different parameter configurations. The COLOR1 line corresponds to a system in the symmetric phase, while the COLOR2 line correspond to the broken phase. The exact parameters for the two configurations are reported under the figure. non si puo parlare di fase rotta e simmetrica. inoltre commenta sulla relazione phi, psibarpsi con lambda=0.
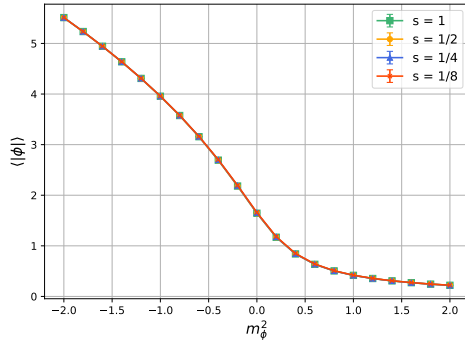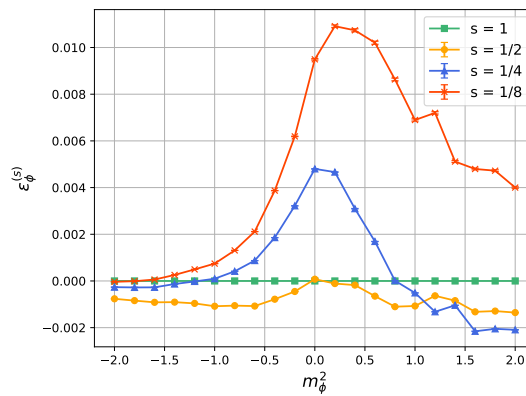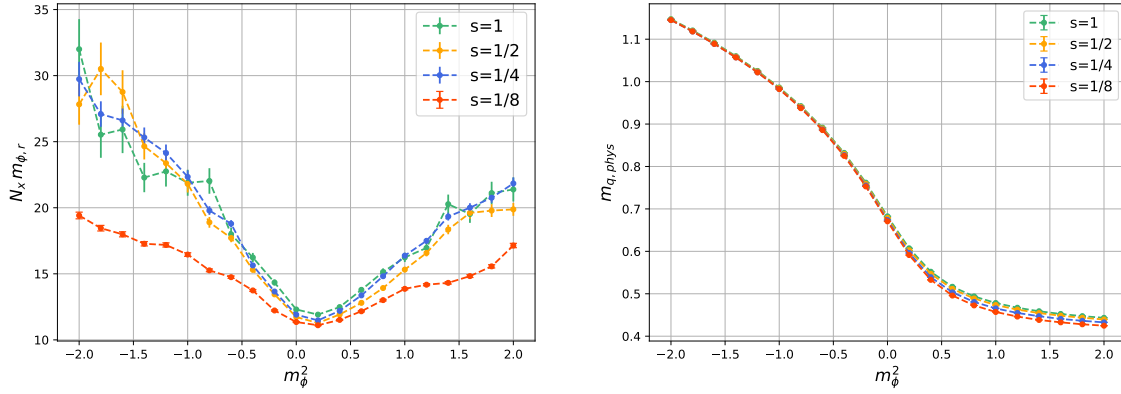
(A) Caption for Image 1
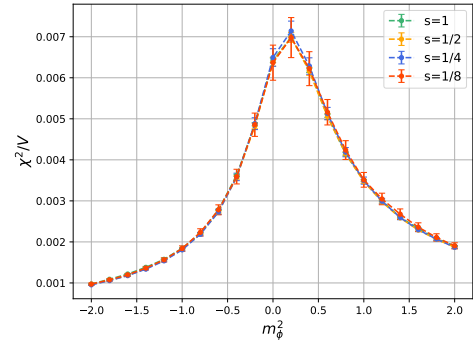
(B) Caption for Image 2
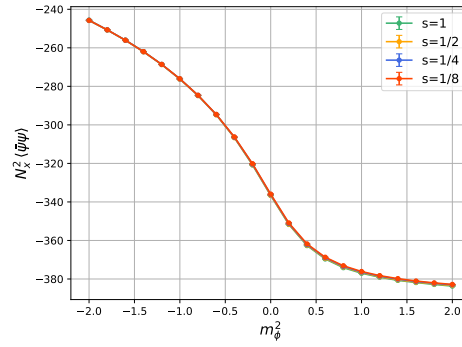
(C) Caption for Image 3

FIGURE 4.5: Overall Caption for the Figure

4.3 Cooling with coloured noise

4.4 Chiral fermions and a glimpse on the chiral phase transition

As explained in section **??**, in the continuum theory chiral symmetry can be broken either explicitly via a finite bare quark mass, or spontaneously if the field gains a non-zero expectation value. Moreoveor, in the discrete formulation, the introduction of the Wilson term also contributes to the explicit breaking of chiral symmetry add reference, as explained in section **??**. This, in particular, means that chiral symmetry is explicitly broken also for $m_q \to 0$. Because of this, one needs a new definition for bare mass M_q, which takes into account the Wilson term contribution, such that chiral symmetry is restored in the limit $M_q \to 0$ for vanishing expectation value of the field ϕ. A convenient way to define such M_q is the following. SSB chiral symmetry $\to$ 3 goldstone massless bosons, the pions. If the bare quark mass is zero, the physical mass of the pions has to be zero. Hence one can extract this mass on the lattice and tune m_q such that this is zero. While this is the correct way to proceed, it is very time takin since one must do mass scans and extrapolations close to singular Dirac operator. This is not the way we pursue here. Instead here we just consider naive fermions and take the limit $m_q \to 0$. This represents a physical theory with $2N_f = 4$ degenerate quarks. This is just done for the purpose of showing some interest properties of coloured noise and not (yet) to match any physical result.

In figure **??** some observables are reported as a function of the noise fraction s for different values of the bare quark mass. In the classical theory ($s = 0$) the order parameters $\langle |\phi| \rangle$, $\langle \bar{\psi}\psi \rangle$ are, in absolute value, bigger than in the quantum case ($s = 1$). As the chiral limit is approached $m_q \to 0$, the figure shows that the classical system lies in the broken phase, while in the quantum settings the symmetry is restored. Discuss general phase structure looking at both ϕ and $\bar{\psi}\psi$. One can see that as m_q is reduced, the systems shifts from a crossover to a second order phase transition, ahighligthed by the susceptibility χ^2 and the binder parameter U_L.

   This would be better discussed as a function of bare scalar mass:
The difference gets more sharped as the base mass decreases, since the theory is closer to the chiral limit discussed above, which corresponds to the case $m_q = 0$. In this limit the systems goes under a second phase transition, highlighted by a peak in the susceptibility and and abrubt change in the Binder cumulant. In contrast, for finite mass, there is smooth crossover where the order parameters change continuously.
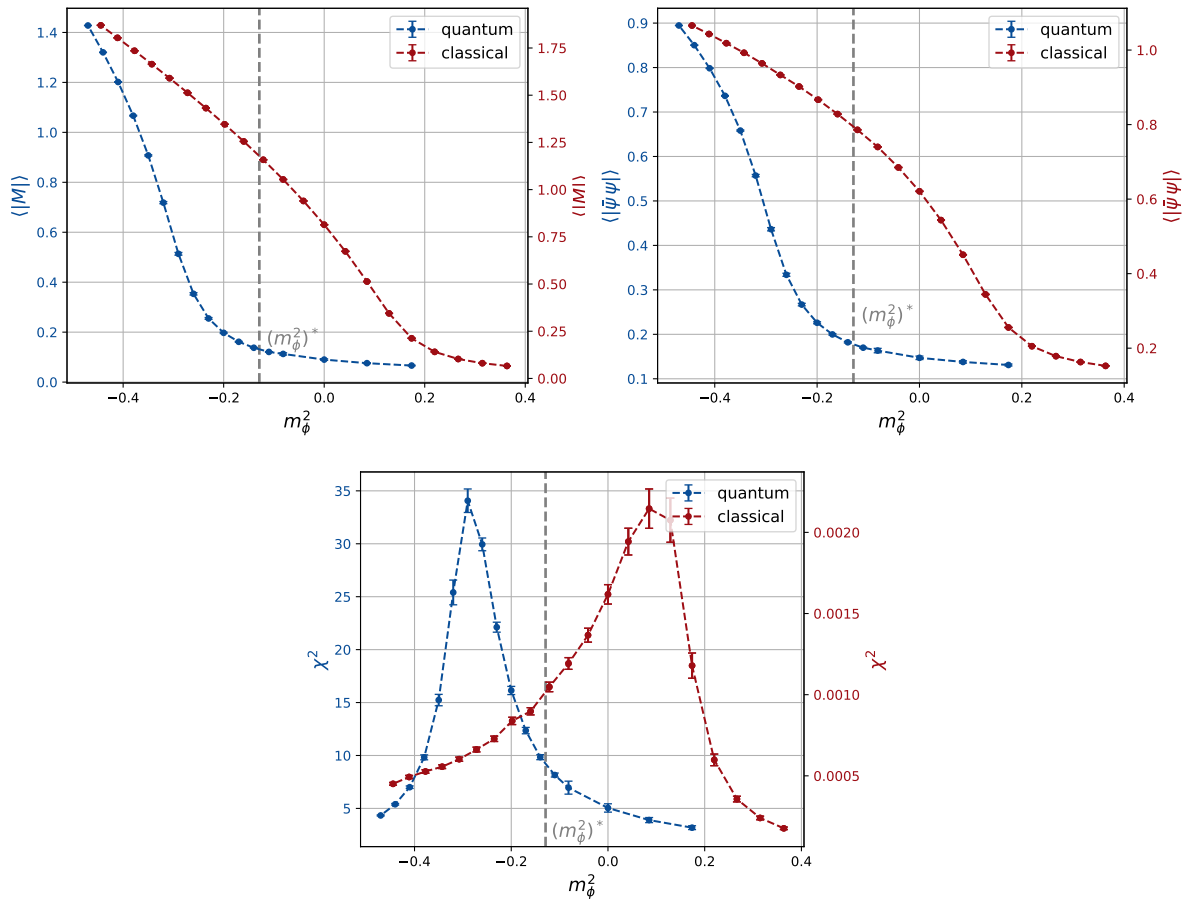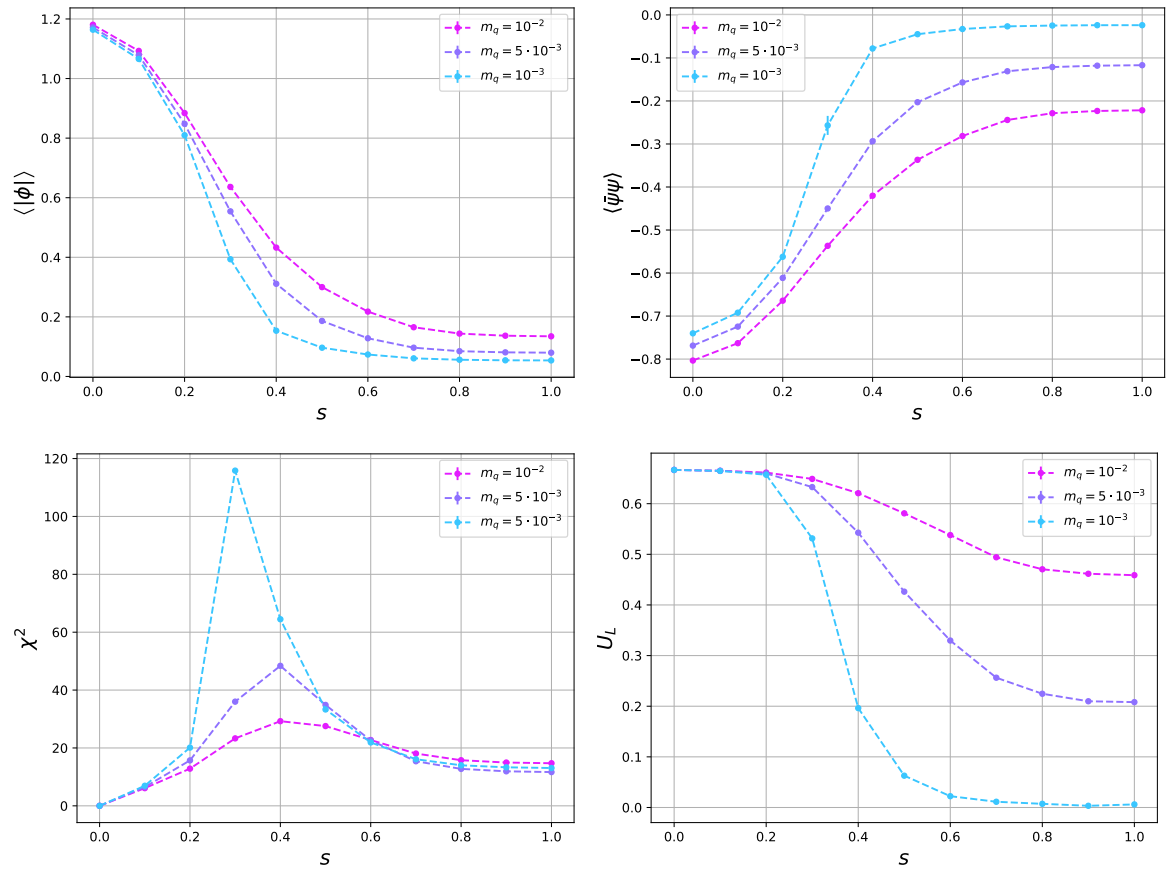
FIGURE 4.6: Chiral symmetry breaking

Chapter 5

Conclusions and outlook

Appendix A

Useful relations and definitions

In this appendix, useful relations and definitions are introduced.

Effective action

$$S_{\text{eff}} = S_\phi + \text{Tr} \log D(\phi)$$

Drift force

$$K_{\phi^j} = -\frac{\delta S}{\delta \phi^j} = -\frac{\delta S_\phi}{\delta \phi^j} - \text{Tr}\left[D^{-1}\frac{\delta D}{\delta \phi^j}\right]$$

Appendix B

Wilson fermions

I am not really sure on whether to put this appendix or not, maybe I will just cite some papers that talk about Wilson fermions

choice of the basis

Appendix C

Algorithms and technical details

cite also felipe for bilinear

C.1 Conjugate Gradient algorithm and the Dirac operator

The full inversion of the Dirac operator is a very expensive computation, given that the Dirac operator has dimension $(2 N_t N_x N_f)^2$, even though it is very sparse and has only few non-zero entries. One can note that for the purpose of computing the fermionic contribution to the drift force and the extraction of the physical quark mass from the correlator (details in section x and section y), only the inverse operator applied to a vector is needed. Hence it is sufficient to compute

$$\psi = D^{-1} |\eta\rangle \tag{C.1}$$

Computing ψ via equation (C.1) is equivalent to solve the linear system $D\psi = \eta$, which can be done efficiently by employing a method for sparse matrices such as Conjugate Gradient (CG) as explained in the following way.

We want to solve the equation

$$D \psi = \eta$$

CG requires the matrix to be hermitian while D is only γ^5-hermitian (really? under which assumptions?). One can thus solve the linear system

$$\left(DD^\dagger\right) \xi = \eta$$

and then obtain ψ by multiplying the solution ξ by $D^\dagger$ since

$$D^\dagger \xi = D^\dagger \left(DD^\dagger\right)^{-1} \eta = D^{-1}\eta = \psi \tag{C.2}$$

Analogously one can calculate

$$\chi = D^\dagger \eta$$

by solving

$$\left(D^\dagger D\right) \xi = \eta$$

and then applying D to the result.

One can improve the solution via CG by solving a *preconditioned* equation. Suppose that we want to solve the equation

$$Mx = b$$

via CG.

Let us express the matrix A as a block matrix

$$M = \begin{pmatrix} A & B \\ C & D \end{pmatrix} \tag{C.3}$$

We introduce the Schur complement of M

$$M/D = A - BD^{-1}C \tag{C.4}$$

This allows one to write M (LDU decomposition, Gaussian elimination) as

$$M = \begin{bmatrix} A & B \\ C & D \end{bmatrix} = \begin{bmatrix} \mathbf{1}_p & -BD^{-1} \\ 0 & \mathbf{1}_q \end{bmatrix} \begin{bmatrix} M/D & 0 \\ 0 & D \end{bmatrix} \begin{bmatrix} \mathbf{1}_p & 0 \\ D^{-1}C & \mathbf{1}_q \end{bmatrix} = LAR$$

Which allows for an easy block inversion

$$M^{-1} = \begin{bmatrix} I_p & 0 \\ -D^{-1}C & I_q \end{bmatrix} \begin{bmatrix} (A - BD^{-1}C)^{-1} & 0 \\ 0 & D^{-1} \end{bmatrix} \begin{bmatrix} I_p & -BD^{-1} \\ 0 & I_q \end{bmatrix} = L^{-1}A^{-1}R^{-1}$$

The equation to solve now reads

$$x = L^{-1}A^{-1}R^{-1}b \qquad \text{or} \qquad y = A^{-1}c$$

with $y = Lx$ and $c = R^{-1}b$. One can then solve the equation $y = A^{-1}c$ and get the solution x by applying L^{-1} to x.

An example of preconditioning is the even-odd preconditioning. Let us write the dirac operator in the form of equation (C.3) in the following way

$$M = \begin{pmatrix} M_{ee} & M_{eo} \\ M_{oe} & M_{oo} \end{pmatrix}$$

The Schur complement (C.4) is

$$\hat{M} \equiv M/M_{oo} =$$

C.2 Bilinear noise scheme

$$\text{Tr}\left[D^{-1} \frac{\delta D}{\delta \phi^j} \right] \approx \langle \eta | D^{-1} \frac{\delta D}{\delta \phi^j} | \eta \rangle = \langle \psi | \frac{\delta D}{\delta \phi^j} | \eta \rangle \qquad | \psi \rangle = D^{-1} | \eta \rangle = D^{\dagger} \underbrace{(DD^{\dagger})^{-1} | \eta \rangle}_{\text{CG}}$$

$$\text{Tr } A = \frac{1}{N} \lim_{N \to \infty} \sum_i^N \eta_i^T D_{ij} \eta_j \tag{C.5}$$

where η_i is a gaussian random field where each component is drawn from a normal distribution $\mathcal{N}(0,1)$.

More precisely each vector component η_i^α satisfies

$$\langle \eta_i^\alpha \rangle = 0 \qquad \left\langle \eta_i^\alpha \eta_j^\beta \right\rangle = \delta_{i,j} \, \delta^{\alpha\beta}$$

The series (C.5) requires in principle an infinite number of vectors to evaluate the trace exactly. In practice we truncate it and choose $N = 1$:D :D. The average over Monte Carlo samples will eventually converge nevertheless to the right result.

Bibliography

[1] L. D. Landau. "On the theory of phase transitions". In: *Zh. Eksp. Teor. Fiz.* 7 (1937). Ed. by D. ter Haar, pp. 19–32. DOI: 10.1016/B978-0-08-010586-4.50034-1.

[2] Vitaly L. Ginzburg. "On Superconductivity and Superfluidity (What I Have and Have Not Managed to Do), as well as on the 'Physical Minimum' at the Beginning of the 21st Century". In: *ChemPhysChem* 5.7 (2004), pp. 930–945. DOI: https://doi.org/10.1002/cphc.200400182. eprint: https://chemistry-europe.onlinelibrary.wiley.com/doi/pdf/10.1002/cphc.200400182. URL: https://chemistry-europe.onlinelibrary.wiley.com/doi/abs/10.1002/cphc.200400182.

[3] Tian Yu Cao, ed. *Conceptual foundations of quantum field theory. Proceedings, Symposium and Workshop, Boston, USA, March 1-3, 1996*. Cambridge, UK: CUP, 1999.

[4] Leo P. Kadanoff. "Scaling laws for ising models near T_c". In: *Physics Physique Fizika* 2 (6 June 1966), pp. 263–272. DOI: 10.1103/PhysicsPhysiqueFizika.2.263. URL: https://link.aps.org/doi/10.1103/PhysicsPhysiqueFizika.2.263.

[5] Kenneth G. Wilson. "Renormalization Group and Critical Phenomena. I. Renormalization Group and the Kadanoff Scaling Picture". In: *Phys. Rev. B* 4 (9 Nov. 1971), pp. 3174–3183. DOI: 10.1103/PhysRevB.4.3174. URL: https://link.aps.org/doi/10.1103/PhysRevB.4.3174.

[6] Kenneth G. Wilson. "Renormalization Group and Critical Phenomena. II. Phase-Space Cell Analysis of Critical Behavior". In: *Phys. Rev. B* 4 (9 Nov. 1971), pp. 3184–3205. DOI: 10.1103/PhysRevB.4.3184. URL: https://link.aps.org/doi/10.1103/PhysRevB.4.3184.

[7] Kenneth G. Wilson and Michael E. Fisher. "Critical Exponents in 3.99 Dimensions". In: *Phys. Rev. Lett.* 28 (4 Jan. 1972), pp. 240–243. DOI: 10.1103/PhysRevLett.28.240. URL: https://link.aps.org/doi/10.1103/PhysRevLett.28.240.

[8] John Cardy. "The renormalization group idea". In: *Scaling and Renormalization in Statistical Physics*. Cambridge Lecture Notes in Physics. Cambridge University Press, 1996, pp. 28–60. DOI: 10.1017/CBO9781316036440.004.

[9] Michael E. Peskin and Daniel V. Schroeder. *An Introduction to quantum field theory*. Reading, USA: Addison-Wesley, 1995. ISBN: 978-0-201-50397-5.

[10] Kenneth G. Wilson and J. Kogut. "The renormalization group and the ϵ expansion". In: *Physics Reports* 12.2 (1974), pp. 75–199. ISSN: 0370-1573. DOI: https://doi.org/10.1016/0370-1573(74)90023-4. URL: https://www.sciencedirect.com/science/article/pii/0370157374900234.

[11] Andrea Carosso. *Novel Approaches to Renormalization Group Transformations in the Continuum and on the Lattice*. 2020. arXiv: 2006.07481 [hep-lat].

[12] Michel Le Bellac. *Thermal Field Theory*. Cambridge Monographs on Mathematical Physics. Cambridge University Press, 1996. DOI: 10.1017/CBO9780511721700.

[13] Heinz J Rothe. *Lattice Gauge Theories*. 4th. WORLD SCIENTIFIC, 2012. DOI: 10.1142/8229. URL: https://www.worldscientific.com/doi/abs/10.1142/8229.

[14] Erhard Seiler. "The case against asymptotic freedom". Applications of RG Methods in Mathematical Sciences. 2003.

[15] Sacha Friedli and Yvan Velenik. *Statistical Mechanics of Lattice Systems: A Concrete Mathematical Introduction*. Cambridge University Press, 2017. DOI: 10.1017/9781316882603.

[16] G. Parisi and Y.-S. Wu. "Perturbation Theory without Gauge Fixing". In: *Scientia Sinica* (24 1981), p. 483.

[17] Poul H. Damgaard and Helmuth Hüffel. "Stochastic quantization". In: *Physics Reports* 152.5-6 (Aug. 1987), pp. 227–398. ISSN: 0370-1573. DOI: 10.1016/0370-1573(87)90144-X.

[18] Crispin Gardiner. *Stochastic Methods: A Handbook for the Natural and Social Sciences*. Springer Berlin, Heidelberg, 2009, pp. XVIII, 447.

[19] Jan M. Pawlowski, Ion Olimpiu Stamatescu, and Felix P.G. Ziegler. "Cooling stochastic quantization with colored noise". In: *Physical Review D* 96.11 (2017). ISSN: 24700029. DOI: 10.1103/PhysRevD.96.114505.

[20] Matthew Schwartz. *Quantum Field Theory and the Standard Model*. Ed. by Cambridge: Cambridge University Press. 2013. DOI: doi:10.1017/9781139540940.

[21] Christof Gattringer and Christian B. Lang. *Lattice quantum chromodynamics*. DOI: 10.1036/1097-8542.yb100080. URL: https://doi.org/10.1036%2F1097-8542.yb100080.

[22] Alejandro Ayala et al. *QCD phase diagram in a magnetized medium from the chiral symmetry perspective: the linear sigma model with quarks and the Nambu–Jona-Lasinio model effective descriptions*. 2021. DOI: 10.1140/epja/s10050-021-00534-4.

[23] Aneesh Manohar and Howard Georgi. "Chiral quarks and the non-relativistic quark model". In: *Nuclear Physics B* 234.1 (1984), pp. 189–212. ISSN: 0550-3213. DOI: https://doi.org/10.1016/0550-3213(84)90231-1. URL: https://www.sciencedirect.com/science/article/pii/0550321384902311.

[24] Michael Creutz. *Quarks, Gluons and Lattices*. Cambridge Monographs on Mathematical Physics. Cambridge University Press, 2023. DOI: 10.1017/9781009290395.

[25] Istvan Montvay and Gernot Münster. *Quantum Fields on a Lattice*. 1994. DOI: 10.1017/cbo9780511470783.

[26] Kenneth G. Wilson. "Confinement of quarks". In: *Phys. Rev. D* 10 (8 Oct. 1974), pp. 2445–2459. DOI: 10.1103/PhysRevD.10.2445. URL: https://link.aps.org/doi/10.1103/PhysRevD.10.2445.

[27] G. G. Batrouni et al. "Langevin simulations of lattice field theories". In: *Phys. Rev. D* 32 (10 Nov. 1985), pp. 2736–2747. DOI: 10.1103/PhysRevD.32.2736. URL: https://link.aps.org/doi/10.1103/PhysRevD.32.2736.

[28] Andreas S. Kronfeld. "Dynamics of Langevin simulations". In: *Prog. Theor. Phys. Suppl.* 111 (1993), pp. 293–312. DOI: 10.1143/PTPS.111.293. arXiv: hep-lat/9205008.

[29] Virginia Vassilevska Williams et al. *New Bounds for Matrix Multiplication: from Alpha to Omega*. 2023. arXiv: 2307.07970 [cs.DS].

[30] Haim Avron and Sivan Toledo. "Randomized Algorithms for Estimating the Trace of an Implicit Symmetric Positive Semi-Definite Matrix". In: *J. ACM* 58.2 (Apr. 2011). ISSN: 0004-5411. DOI: 10.1145/1944345.1944349. URL: https://doi.org/10.1145/1944345.1944349.

[31] Werner Horsthemke. "Noise Induced Transitions". In: *Non-Equilibrium Dynamics in Chemical Systems*. Ed. by Christian Vidal and Adolphe Pacault. Berlin, Heidelberg: Springer Berlin Heidelberg, 1984, pp. 150–160. ISBN: 978-3-642-70196-2.

[32] Raúl Toral. "Noise-induced transitions vs. noise-induced phase transitions". In: *AIP Conference Proceedings* 1332.1 (Mar. 2011), pp. 145–154. ISSN: 0094-243X. DOI: 10.1063/1.3569493. eprint: https://pubs.aip.org/aip/acp/article-pdf/1332/1/145/12109027/145_1_online.pdf. URL: https://doi.org/10.1063/1.3569493.

[33] Yousef Saad. *Iterative Methods for Sparse Linear Systems*. Second. Society for Industrial and Applied Mathematics, 2003. DOI: 10.1137/1.9780898718003. eprint: https://epubs.siam.org/doi/pdf/10.1137/1.9780898718003. URL: https://epubs.siam.org/doi/abs/10.1137/1.9780898718003.

List of Abbreviations

RG   **R**enormalisation **G**group
fRG   Functional **R**enormalisation **G**group
UV   **U**ltraviolet
QFT   **Q**uantum **F**ield **Theory**

Physical Constants

Speed of Light $\quad c_0 = 2.997\,924\,58 \times 10^8\,\mathrm{m\,s^{-1}}$ (exact)

List of Symbols